Feasibility of a silicon thin film transistor-based aptamer sensor for COVID-19 detection

Thomas Farrow
Department of Electrical Engineering and Electronics, University of Liverpool
Siriny Laumier
Department of Electrical Engineering and Electronics, University of Liverpool
Steve Hall
Department of Electrical Engineering and Electronics, University of Liverpool
Ian Sandall
Department of Electrical Engineering and Electronics, University of Liverpool
Harm van Zalinge (vzalinge@liverpool.ac.uk)
Department of Electrical Engineering and Electronics, University of Liverpool https://orcid.org/0000-0003-0996-1281

Research Article

Keywords: Biosensors, Thin film sensors, Thin film transistors

Posted Date: December 3rd, 2020

DOI: https://doi.org/10.21203/rs.3.rs-74726/v2

Feasibility of a silicon thin film transistor-based aptamer sensor for COVID-19 detection

Thomas Farrow, Siriny Laumier, Steve Hall, Ian Sandall and Harm van Zalinge

***Abstract*— Since the beginning of the coronavirus disease 2019 (COVID-19) in December 2019 and the current lack to date of specific drugs or vaccinations to cope with the disease, it has become apparent that the surest way of dealing with this is through early diagnosis and management. Current testing has shown to be unable to rapidly and accurately provide the results required to restrict the spread. Here we report feasibility for the use of an intrinsic silicon thin film transistor functionalised with aptamers designed to attach to the spike protein of COVID-19. It is shown that a linear response can be obtained in a concentration range of 1 pM to 1 nM.**

***Index Terms*— Biosensors, Thin film sensors, Thin film transistors**

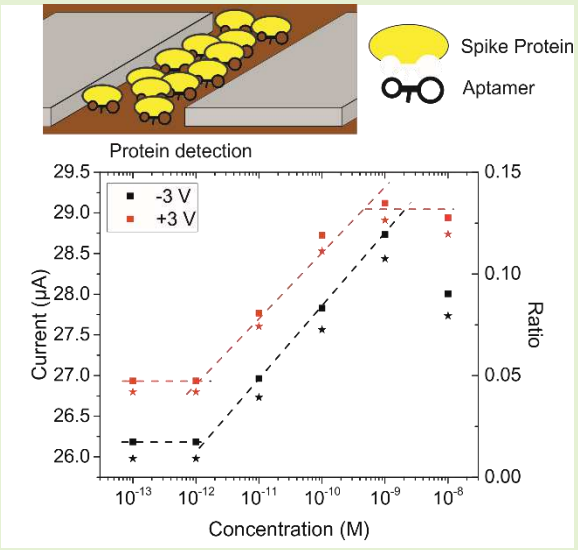

I. Introduction

In December 2019, a number of unusual cases of pneumonia of unknown origin were reported in Wuhan in the Hubei province of China [1]. This was subsequently identified as the novel coronavirus (2019-nCov) and renamed severe acute respiratory syndrome coronavirus 2 (SARS-CoV2) by the International Committee on Taxonomy of Viruses [2]. From early 2020 human-to-human transmission has accelerated the spread of the virus across the world, resulting in the World Health Organisation (WHO) declaring the COVID-19 outbreak as a pandemic in March 2020. By late November 2020 the number of confirmed cases is approaching 60 million and over 1.4 million deaths related from COVID-19 world-wide are reported [3]. During the first six months of 2020, nearly all countries have imposed lockdowns and restrictions upon their citizens to slow the spread of COVID-19 to manageable levels and prevent health services from being overwhelmed. While the severity of these lockdowns and restrictions vary between countries, governments which have deployed mass rapid testing of citizens have generally required less severe restrictions and have appeared to be able to manage outbreaks with fewer cases and fatalities.

Traditionally the presence of viruses has been determined by culture followed by observation. Although the advantages of this technique are that it is cheap and has high specificity, problems arise in that the samples need to be taken from the infected area. In order to address these issues, two different types of detection methods have been developed. The first is the so-called antigen testing. The second method is based on molecular based detection [4]. One such of the latter technique is polymerase chain reaction (PCR) which is used to amplify the quantity of species-specific genes unique to a disease. While PCR has been used as the gold standard testing method for COVID-19 monitoring, it is time-consuming requiring dedicated laboratories, bespoke equipment and trained personnel, making it non-ideal for the level of mass testing that is required for COVID-19. As such there is a need to develop faster and simpler testing, whilst maintaining the selectivity and sensitivity offered by PCR.

SARS-CoV2 is highly similar to the SARS virus attributed to the outbreak in 2003 [5]. In general a mature COVID-19 virus has polyprotein, four structural and five accessary proteins [6]. The polyprotein is the open reading frame 1a and 1b, Orf1ab, while the structural proteins are the envelope protein, E, membrane protein, M, nucleocapsid protein, N, and the spike protein, S. The accessary proteins are Orf3a, Orf6, Orf7a, Orf8

This paragraph of the first footnote will contain the date on which you submitted your paper for review

T. Farrow, S. Laumier, I. Sandall and H. van Zalinge are all with the Department of Electrical Engineering and Electronics, University of Liverpool, Brownlow Hill, Liverpool, L69 3GJ, United Kingdom.

T.F. and S.L. contributed equally as first author.

I.S. and H.v.Z. are corresponding authors (isandall@liverpool.ac.uk and vzalinge@liverpool.ac.uk)

and Orf10. The Orf1ab protein causes the viral RNA replication and transcription [6]. Proteins E and M are responsible for the viral assembly of the coronavirus, while protein N is required for the viral RNA synthesis [7]. Protein S sits on the surface of the viral particle and facilitates the infection of host cells by binding to its receptor, ACE2, via the receptor binding domain of the protein. This protein is also the only one that is significantly different to those found in the original SARS-CoV-1 [8].

Over recent years, the so-called immuno-FET, has been demonstrated as a potential low-cost bio-sensor platform. An immuno-FET is a standard thin film transistor in which the gate is replaced by a layer of antibodies specific for the target protein [9, 10]. Once the target is attached to the antibody, the charged areas of the protein will cause an electrostatic change in the conduction channel of the FET and hence modulate the source-drain current. Such a device and concept has already been demonstrated for potential COVID-19 detection [11].

Currently a major limitation in the performance of immuno-FETs is the screening effect when employed in physiological fluids [12]. The ions present in the solution cause the formation of a double layer with a thickness equal to the Debye length. Any change in the charge distribution outside this layer will not affect the conduction channel of the FET. For a standard salt concentration of 0.1 M, the Debye length is approximately 1 nm. As the antibodies have a size of roughly 10 nm the target protein cannot be detected by the immuno-FET.

In recent years, a new group of molecules has been developed. These so-called aptamers consist of short DNA, RNA or peptide strands [13, 14]. Utilising their conformation and charge distribution, aptamers are capable of very specific binding to individual proteins. As they are significantly smaller than the antibodies, the result is that a protein bound via an aptamer to the conduction channel will create the required change in the electrical properties at higher salt concentration. This in turn means that it becomes possible to use this system with physiologically relevant liquids. In addition, aptamers are significantly cheaper and more stable than antibodies.

The majority of aptamer based sensors employ electrochemical methods of detection and have been around for over a decade [15]. However, more recently the same technique has been used within the setting of an aptamer FET and has been proved to be effective for a wide range of molecular size. Such sensors can determine the presence of small molecules [16]. On the other side of the molecular size scale it is proven possible to detect the presence of avian influenza in chicken serum [17].

In this paper we explore the feasibility of a simple intrinsic silicon thin film transistor (TFT) functionalised with an aptamer sequence which binds to the spike protein of COVID-19 to be used as sensor. Traditionally aptamer functionalised transistors rely on measuring a single source drain potential to determine the target protein concentration dependency. Our focus is to use a wide range of potentials to obtain a broader concentration dependency not only to optimise the response of the sensor, but also to learn more about the processes that are occurring in the binding of the protein by the aptamer. This is first time that aptamers have been used in a field effect transistor as a binding element for the spike protein of COVID-19.

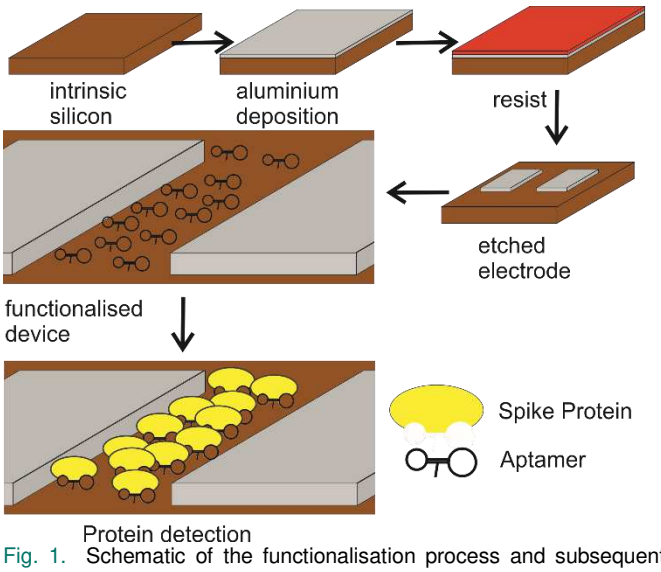

Fig. 1. Schematic of the functionalisation process and subsequent detection of the spike protein.

II. Experimental Methods

The experiments focus on the use of a nominally undoped silicon thin film transistor; the wafer was provided by Miplaza, Philips, The Netherlands. A bottom-up technique has been used to fabricate the electrodes. A layer of 100 nm of aluminium (Puratronic 99.99% purity) was deposited by thermal evaporation on the silicon wafer using a Moorfields evaporator. The device consists of two rectangular electrodes of 1 mm×0.5 mm separated by a gap, which forms the sensor. The gap size was kept constant for all experiments and measured at 50 µm. After spin coating the resist (Shipley, S1813, positive photoresist) Ohmic contact electrodes were patterned using photolithography. Subsequently the undeveloped resist was removed by washing in de-ionised water, followed by an Al etch step (Al etchant from Technic. Inc. used as-received). The final steps were a de-ionised water wash to remove the etchant and etched Al, followed by an acetone wash for the residual resist removal.

All chemicals used for the functionalisation and the subsequent experiments were purchased from Merck and used as-received, unless stated otherwise. The aptamer probe was attached to the silicon channel using a silanisation method [18]. In brief this consisted of immersion in an ethanol solution containing 3% (v/v) APTES at 80 °C for 2 h. After washing the silicon four times with ethanol and deionized water, the samples were dried under N_2, and heated at 110 °C for 1 h. A cross-linker, glutaraldehyde was used to create the binding side for the aptamer. The samples were immersed in a glutaraldehyde/water solution containing 2% (v/v) glutaraldehyde at room temperature (25 ± 2 °C) for 1 h and then rinsed with deionized water, dried under N2. In the final step amine functionalised aptamers, Eurogentec, Belgium, were used. The aptamer solution (200 µL, 100 nM), was incubated at 37 °C for 2 h and then rinsed with PBS and deionized water to

remove the excess aptamers, then dried under N_2. There is a possibility that not all glutaraldehyde free ester groups bind to an aptamer and as such they provide a site that potentially can bind non-specifically to any amine group present in the proteins. Following the aptamer functionalization, the samples were immersed in a PBS solution containing 80 mM glycine for 60 minutes at room temperature and subsequently rinsed in PBS and dried in a N_2 atmosphere.

An aptamer previously reported to bind to the spike protein of the COVID-19 virus was used [19]. The sequence is 5'-CAGCACCGACCTTGTGCTTTGGGAGTGCTGGTCCAAG GGCGTTAATGGACA-3'. The aptamer was functionalised with an amine terminal group at the 5' end. Once the samples have been functionalised, the response to varying concentrations of the recombinant SARS-CoV-2 spike protein, S1 Subunit [20], Cambridge Bioscience, UK, was determined with serial dilutions of the spike protein in PBS. Prior to any characterisation the samples were exposed to a PBS solution without the protein. The samples were left in the solutions for 15 minutes and subsequently washed with PBS and blown dry with N2. A schematic representation of the functionalisation process is shown in Figure 1.

In the following experiments and the subsequent discussions the spike protein that is bound to the surface is assumed to create a potential similar to that of a gate voltage, through the presence of differently charged areas within the protein. This results in modulation of current through the TFT.

III. Results and Discussion

Consider first the thin film transistor IV-characteristics without functionalization, as shown in Figure 2a. The Al Ohmic contacts are seen to be weakly rectifying and the final regime at high voltage shows a quasi-saturation of the current indicating pinch-off of the channel as expected in field-effect transistor characteristics. The inset show the data on a log-log plot. Three different regimes are apparent. The first regime at low voltages (<0.1V) has a slope of approximately 1 indicating ohmic conduction; the weakly rectifying region is approximately linear over the small range of voltage. This is followed by a region with a slope equal to 2.4, close to a quadratic dependence and in the final pinch-off region the slope decreases to 0.3, the saturation region.

Consider next the addition of the functionalization layers and the spike protein. The shape of the curve does not change significantly as seen in Figure 2b. The conduction is still seen to be determined by the standard TFT behavior. Comparing the double logarithmic slopes of the different regions, data shown in Table S1, supplementary information, as indicated in Figure S1, the linear region is the same for all sweeps. Upon the addition of the functionalisation and the subsequent addition of the spike protein in the pre-saturation region, the slope decreases from 2.4 to 2.1. In the final saturation region of the TFT the slope increases by 50% from 0.3 on the bare silicon TFT to 0.45 on the functionalized devices. However, no

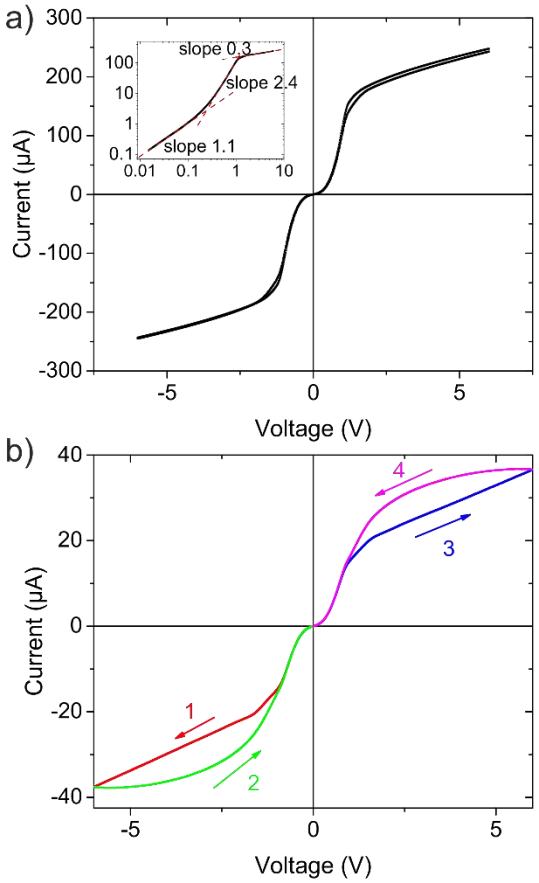

Fig. 2. IV characteristics of the bare silicon TFT (a) and functionalised with the silane and aptamer layer but without the spike protein (b). The inset in a) show the IV characteristics on a double logarithmic scale, also indicated are the different slopes. The arrows and numbers in b) indicate the sequence and direction of the voltage sweeps. The insert shows the electric field distribution during the sweeps 3 and 4.

dependence of the various slopes on the spike protein concentration is evident.

An additional change after functionalization can be seen in the more marked hysteresis as shown in Figure 2b. The voltage sweep follows the arrows as indicated in the graph. It is proposed that the observed effect can be explained by slow moving ions that are present on the surface [21]. During the initial sweeps starting from 0 to ±6 V, ions present in the organic film created in the functionalization and the subsequent steps, will move in accordance to their charge polarity under the action of the increasing source to drain electric field. This is an inherent slow process due to the low mobility of the ions and as a result their redistribution will not significantly affect the electric field. However, on the return sweep from ±6 V to 0, the ions are concentrated towards one end of the device serving to modulate the channel charge and hence the current.

In Figure 3a, the IV-characteristics at various concentrations of the spike protein ranging from 0 to 10 nM in PBS are shown. The return sweeps affected by the hysteresis are omitted for clarity, however similar behavior as discussed above is seen at all concentrations.

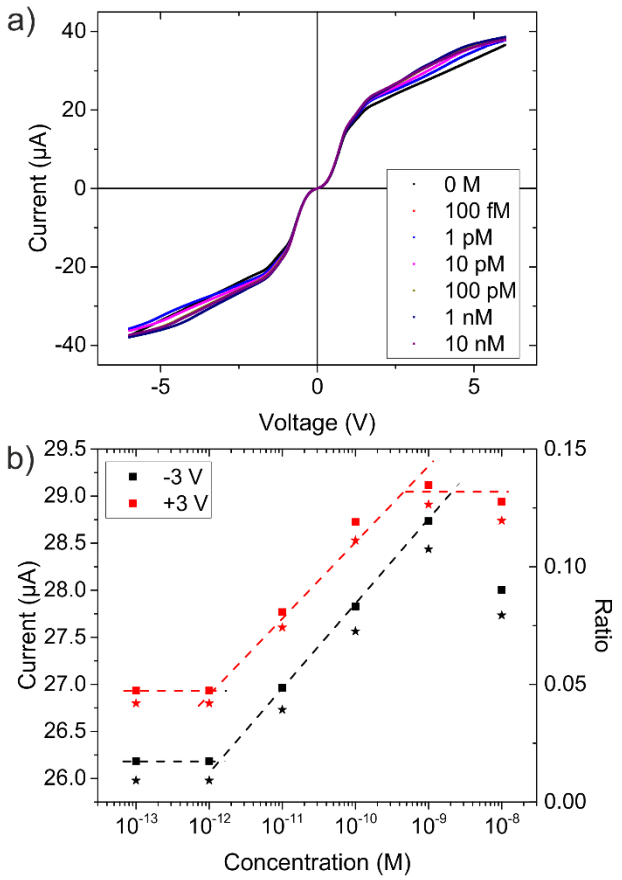

Fig. 3 In a) the IV characteristics are shown for different concentrations of the spike protein ranging from 0 to 10 nM. In b) the absolute value of the current (squares), and the ratio (asterisks) at -3 V (black) and +3 V (red) is shown. The dashed lines are a guide for the eye only and indicate the behaviour of the sensor as a function of the spike protein concentration.

We introduce a parameter, R, to facilitate analysis of the output without the need to account for minor fluctuations due to the fabrication process. The parameter is defined as the relative change and is given in Eqn.1 below

$$R = \frac{I - I_0}{I_0} \quad (1)$$

where I, is the measured current and I_0 is that measured at the same voltage in the IV characteristic without the presence of the target protein. The values for both the current and R at ±3 V are shown in Figure 3b. A constant difference can be seen between the positive and the negative voltages, however, the overall behavior is identical. At low concentration, up to 1 pM, of spike protein the sensor is not sensitive enough to detect the presence of the protein. At concentrations above 1 nM, the sensor saturates. However, in between there is a concentration range within which the device shows a linear response to changes in concentration. Although not shown, it is worth noting that at all potentials used within this study a similar curve with the same characteristics of both the current and ratio can be observed.

Sixteen devices were tested and the results presented here are considered to be representative of this sample (see supplementary information Figure S2 and Table S2). Referring to Fig. 3b, the current increases within the linear range as (0.85 ± 0.02) μA, at -3 V, and (0.75 ± 0.08) μA, for 3 V, per decade increase of the concentration with a Pearson correlation of 0.99995 for both. Similar values have been found for the other devices that were examined so the result can be considered typical The ratio changes at a rate of approximately 0.03 (± 0.002) per decade change in the concentration, indicating that the aptamer functionalised thin film transistors have the potential to be a sensor capable of detecting spike protein.

The only comparative study that has been reported so far, was that performed using a graphene TFT, where the same spike protein was examined, but using an antibody to obtain the selective binding [11]. There are three major differences in the experimental technique compared to the results presented here. The first is the use of graphene, the second that the experiments were performed in liquid, the third is that an antibody was used for the attachment of the spike protein. Both this study and that of [11], show similar response to the presence of spike protein. In both cases the ratio increases approximately 10% at the maximum spike concentration compared to the 0% response.

IV. Conclusions

In summary, using a known aptamer sequence that binds to the spike protein, we have shown that it is feasible to successfully detect the proteins presence in a thin film intrinsic silicon transistor, with a linear detection range between 1 pM and 1 nM or 0.75 ng/ml to 0.75 μg/ml. The basic sensor shown here is made with a very low-cost, simple process. The study demonstrates the feasible to obtain sufficient sensitivity to facilitate improved integration into a sensory system for Covid-19.

References

[1] World Health Organisation. "Novel Coronavirus(2019-nCoV)SITUATION REPORT-121 JANUARY 2020," https://www.who.int/docs/default-source/coronaviruse/situation-reports/20200121-sitrep-1-2019-ncov.pdf.

[2] A. E. Gorbalenya, S. C. Baker, R. S. Baric *et al.*, "The species Severe acute respiratory syndrome-related coronavirus: classifying 2019-nCoV and naming it SARS-CoV-2," *Nature Microbiology,* vol. 5, no. 4, pp. 536-544, 2020/04/01, 2020.

[3] John Hopkins Institute. "WHO Coronavirus Disease (COVID-19) Dashboard," https://covid19.who.int/?gclid=EAIaIQobChMIr7j6tuyV6wIVWe3tCh17Kws6EAAYASABEgKohPD_BwE.

[4] L. J. Carter, L. V. Garner, J. W. Smoot *et al.*, "Assay Techniques and Test Development for COVID-19 Diagnosis," *ACS Central Science,* vol. 6, no. 5, pp. 591-605, 2020/05/27, 2020.

[5] J. F. W. Chan, K. H. Kok, Z. Zhu *et al.*, "Genomic characterization of the 2019 novel human-pathogenic coronavirus isolated from a patient with atypical pneumonia after visiting Wuhan," *Emerging Microbes and Infections,* vol. 9, no. 1, pp. 221-236, 2020.

[6] K. Narayanan, C. Huang, and S. Makino, "SARS coronavirus accessory proteins," *Virus Research,* vol. 133, no. 1, pp. 113-121, 2008/04/01/, 2008.

[7] D. Schoeman, and B. C. Fielding, "Coronavirus envelope protein: current knowledge," *Virology Journal,* vol. 16, no. 1, pp. 69, 2019/05/27, 2019.

[8] W. Tai, L. He, X. Zhang *et al.*, "Characterization of the receptor-binding domain (RBD) of 2019 novel coronavirus: implication for development of RBD protein as a viral attachment inhibitor and vaccine," *Cellular & Molecular Immunology,* vol. 17, no. 6, pp. 613-620, 2020/06/01, 2020.

[9] F. Patolsky, G. Zheng, O. Hayden *et al.*, "Electrical detection of single viruses," *Proceedings of the National Academy of Sciences of the United States of America,* vol. 101, no. 39, pp. 14017-14022, 2004.

[10] G. J. Zhang, L. Zhang, M. J. Huang *et al.*, "Silicon nanowire biosensor for highly sensitive and rapid detection of Dengue virus," *Sensors and Actuators, B: Chemical,* vol. 146, no. 1, pp. 138-144, 2010.

[11] G. Seo, G. Lee, M. J. Kim *et al.*, "Rapid Detection of COVID-19 Causative Virus (SARS-CoV-2) in Human Nasopharyngeal Swab Specimens Using Field-Effect Transistor-Based Biosensor," *ACS nano,* vol. 14, no. 4, pp. 5135-5142, 2020.

[12] D. P. Tran, M. A. Winter, B. Wolfrum *et al.*, "Toward Intraoperative Detection of Disseminated Tumor Cells in Lymph Nodes with Silicon Nanowire Field Effect Transistors," *ACS Nano,* vol. 10, no. 2, pp. 2357-2364, 2016.

[13] M. Ilgu, and M. Nilsen-Hamilton, "Aptamers in analytics," *Analyst,* vol. 141, no. 5, pp. 1551-1558, 2016.

[14] R. Wilson, C. Bourne, R. R. Chaudhuri *et al.*, "Single-step selection of bivalent aptamers validated by comparison with SELEX using high-throughput sequencing," *PLoS ONE,* vol. 9, no. 6, 2014.

[15] R. J. White, N. Phares, A. A. Lubin *et al.*, "Optimization of Electrochemical Aptamer-Based Sensors via Optimization of Probe Packing Density and Surface Chemistry," *Langmuir,* vol. 24, no. 18, pp. 10513-10518, 2008/09/16, 2008.

[16] N. Nakatsuka, K. A. Yang, J. M. Abendroth *et al.*, "Aptamer-field-effect transistors overcome Debye length limitations for small-molecule sensing," *Science,* vol. 362, no. 6412, pp. 319-324, 2018.

[17] J. Kwon, Y. Lee, T. Lee *et al.*, "Aptamer-Based Field-Effect Transistor for Detection of Avian Influenza Virus in Chicken Serum," *Analytical Chemistry,* vol. 92, no. 7, pp. 5524-5531, 2020.

[18] L. D. Stefano, G. Oliviero, J. Amato *et al.*, "Aminosilane functionalizations of mesoporous oxidized silicon for oligonucleotide synthesis and detection," *Journal of the Royal Society Interface,* vol. 10, no. 83, 2013.

[19] Y. Song, J. Song, X. Wei *et al.*, "Discovery of Aptamers Targeting the Receptor-Binding Domain of the SARS-CoV-2 Spike Glycoprotein," *Analytical Chemistry,* vol. 92, no. 14, pp. 9895-9900, 2020/07/21, 2020.

[20] J. Lan, J. Ge, J. Yu *et al.*, "Structure of the SARS-CoV-2 spike receptor-binding domain bound to the ACE2 receptor," *Nature,* vol. 581, no. 7807, pp. 215-220, 2020/05/01, 2020.

[21] M. Sajedi Alvar, P. W. M. Blom, and G. J. A. H. Wetzelaer, "Space-charge-limited electron and hole currents in hybrid organic-inorganic perovskites," *Nature Communications,* vol. 11, no. 1, 2020.

Figures

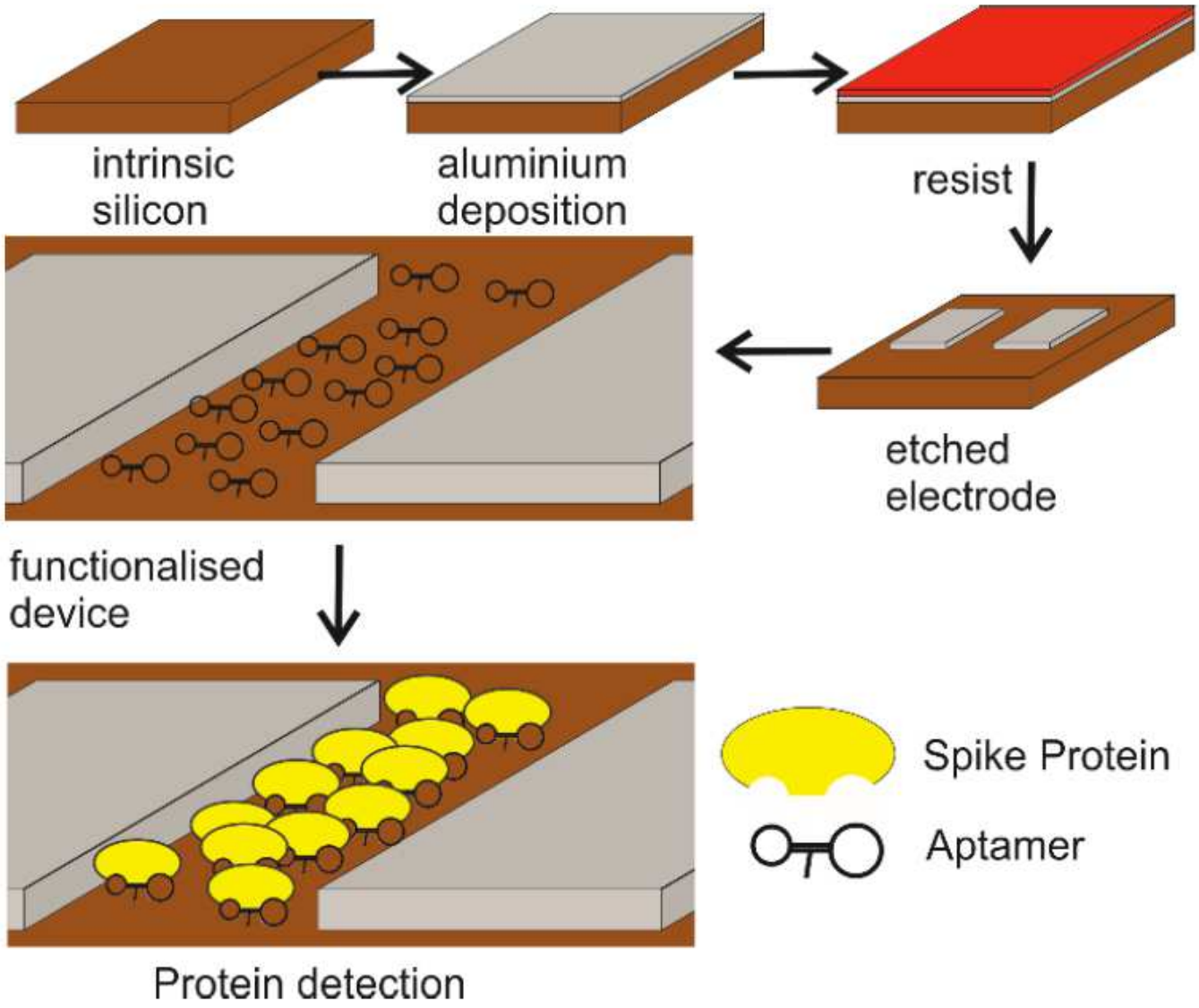

Figure 1

Schematic of the functionalisation process and subsequent detection of the spike protein.

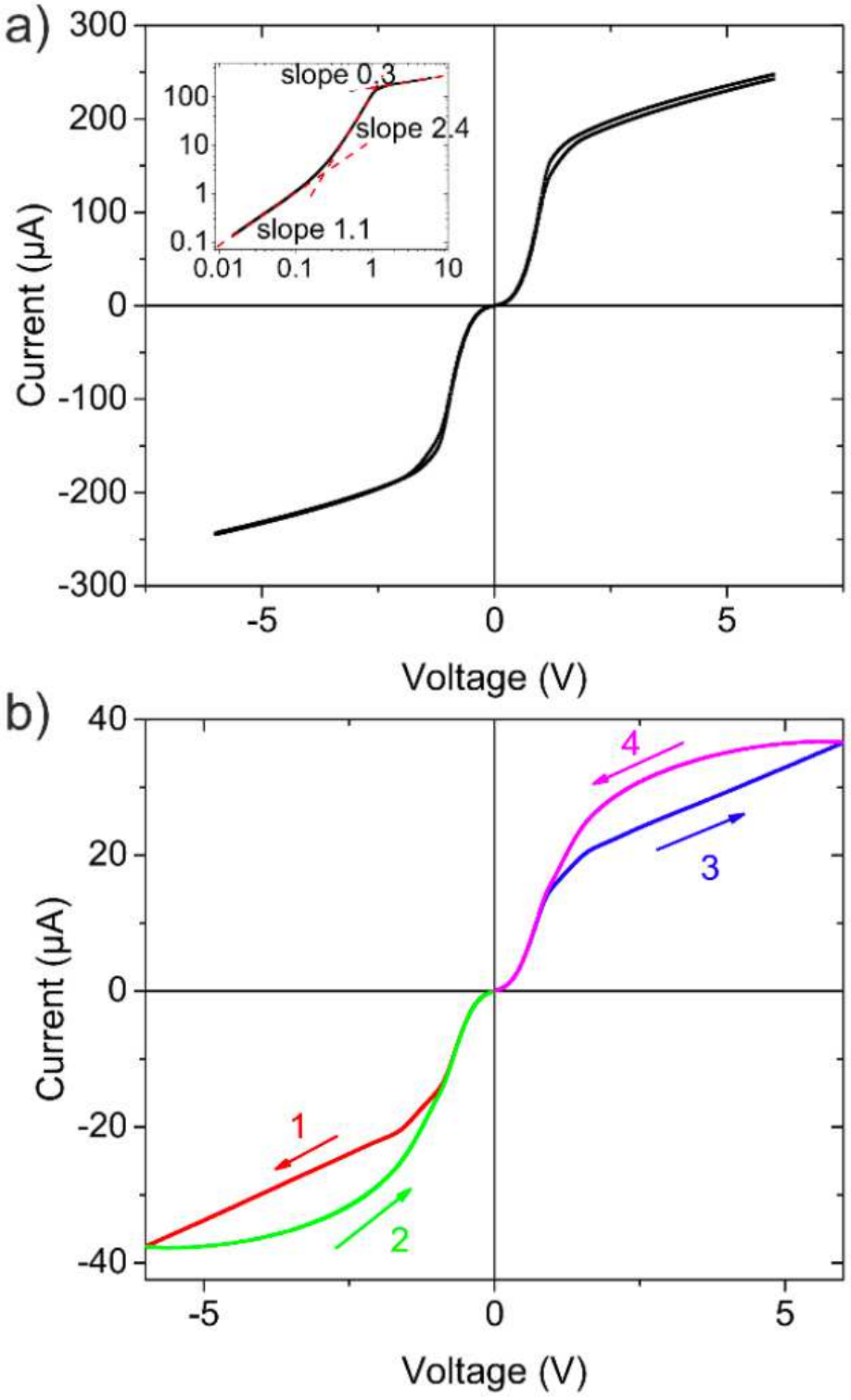

Figure 2

IV characteristics of the bare silicon TFT (a) and functionalised with the silane and aptamer layer but without the spike protein (b). The inset in a) show the IV characteristics on a double logarithmic scale, also indicated are the different slopes. The arrows and numbers in b) indicate the sequence and direction of the voltage sweeps. The insert shows the electric field distribution during the sweeps 3 and 4.

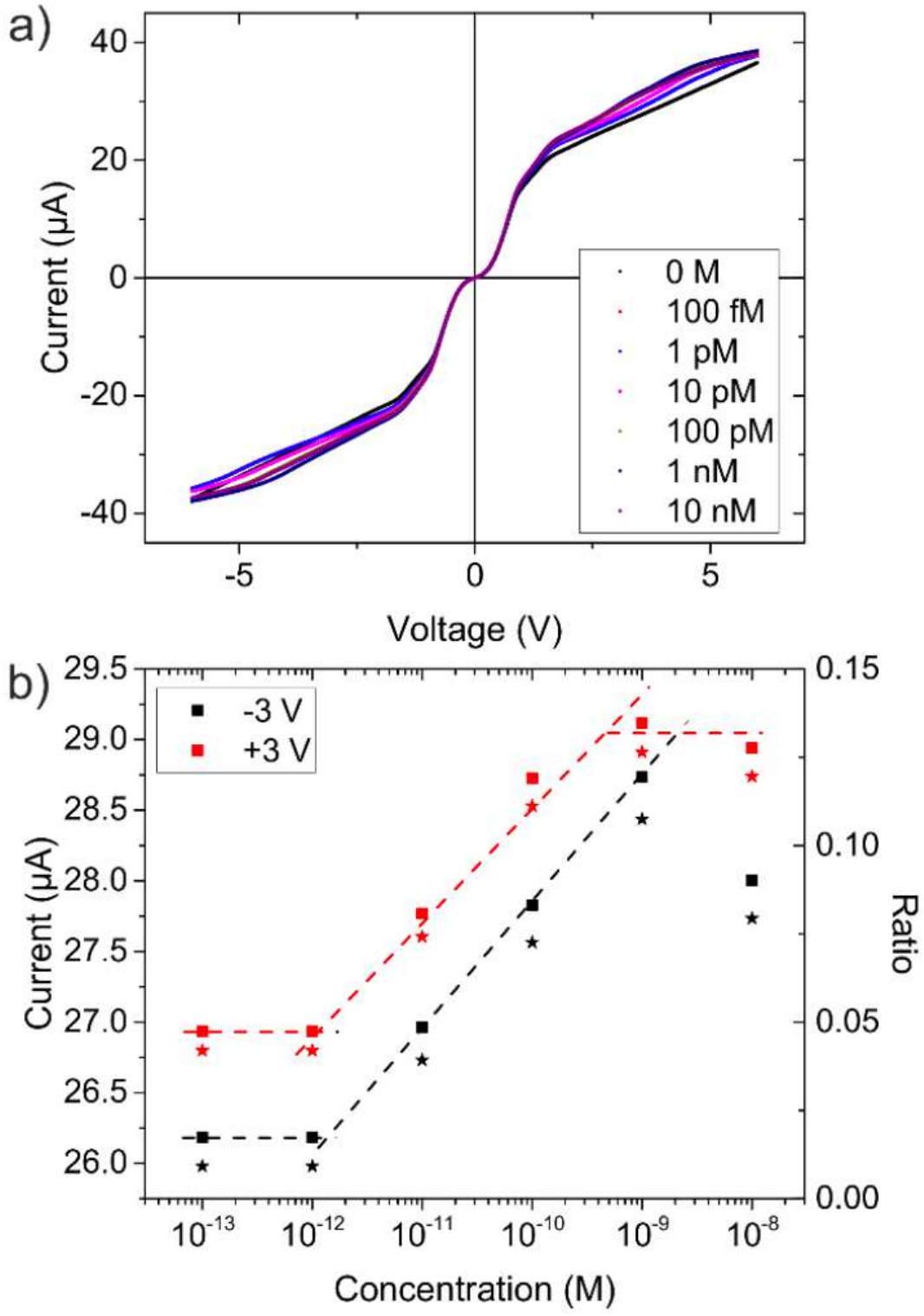

Figure 3

In a) the IV characteristics are shown for different concentrations of the spike protein ranging from 0 to 10 nM. In b) the absolute value of the current (squares), and the ratio (asterisks) at -3 V (black) and +3 V (red) is shown. The dashed lines are a guide for the eye only and indicate the behaviour of the sensor as a function of the spike protein concentration.

Supplementary Files

This is a list of supplementary files associated with this preprint. Click to download.

- AbstractGraphic.png
- FarrowetalSupplementaryInformation.pdf